

## Electrochemical sensing behaviour of nickel oxide nanospheres synthesized from nickel EDTA complex by decomposition method

R. Manigandan<sup>a</sup>, K. Giribabu<sup>a</sup>, R. Suresh<sup>a</sup>, S. Munusamy<sup>a</sup>, S. Praveen Kumar<sup>a</sup>, S. Muthamizh<sup>a</sup>, A. Stephen<sup>b</sup> and V. Narayanan<sup>\*b</sup>

<sup>a</sup>Department of Inorganic Chemistry, University of Madras, Guindy Campus, Chennai-600 025, India

<sup>b</sup>Department of Nuclear Physics, University of Madras, Guindy Campus, Chennai-600 025, India

E-mail : vnnara@yahoo.co.in

---

**Abstract :** We have synthesized nickel oxide (NiO) nanospheres by thermal decomposition method. X-Ray diffraction analysis (XRD), scanning electron microscopy (SEM), and Fourier transform infrared spectroscopy (FT-IR) were used to characterize the synthesized nickel oxide nanospheres. The FT-IR spectrum shows a vibration in the region of  $451\text{ cm}^{-1}$  that confirms the existence of metal-oxygen bond. XRD confirms the structure, crystallinity and phase of the nickel oxide nanospheres. The morphology of the nickel oxide nanospheres was investigated by SEM analysis. Further, the synthesized nickel oxide nanospheres were coated on the glassy carbon electrode (GCE) and the NiO/GCE electrode shows good electrochemical sensing behaviour toward hydrogen peroxide. It shows that the nickel oxide nanospheres exhibit promising applications in the development of sensors.

**Keywords :** Nickel oxide nanospheres, EDTA, sensor, hydrogen peroxide.

---

### Introduction

Metal oxides with nanoscale were most extensively studied due to large surface areas, unusual adsorptive properties, diffusivity, and surface defects<sup>1-3</sup>. Especially NiO can be used as an electrochromic films, magnetic materials, p-type transparent conducting films, gas sensors, catalyst, batteries cathode, capacitor and solid oxide fuel cells anode<sup>4</sup>. In this study, we have reported the synthesis of NiO nanoparticles from Ni-EDTA complex using simple thermal decomposition method. Additionally, the electrochemical sensing property of NiO toward hydrogen peroxide was performed.

### Experimental

Nickel chloride hexahydrate ( $\text{NiCl}_2 \cdot 6\text{H}_2\text{O}$ ), disodium salt of ethylene diamine tetra acetic acid (EDTA), and glycerol, sodium dihydrogen phosphate and disodium hydrogen phosphate were purchased from Qualigens. Double distilled water was used as the solvent throughout the experiment. NiO was prepared by thermal decomposition of nickel EDTA. Nickel EDTA was prepared by reacting aqueous solutions of 0.01 M nickel chloride and 0.01 M disodium salt of EDTA. The 0.1 M nickel chlo-

ride was dissolved in 500 ml distilled water. After 20 min stirring the dissolved EDTA in 50 ml water was slowly added dropwise with constant stirring. This suspension was stirred for 20 min at 50 °C in magnetic stirrer. The obtained nickel EDTA was annealed in air for 3 h at 450 °C to form NiO nanoparticles.

The crystal structure of NiO nanoparticles was analyzed by a Rich Siefert 3000 diffractometer with Cu-K $\alpha$ 1 radiation ( $\lambda = 1.5406\text{ \AA}$ ). FT-IR spectrum of the NiO was recorded on Shimadzu FT-IR 8300 series instrument by using potassium bromide pellets. The surface morphology of the NiO was acquired by SEM HITACHI SU6600 scanning electron microscopy respectively. Ultrasonically dispersed NiO nanopowder in 5 mL of water was drop coated onto the GCE and dried at room temperature. The NiO coated electrode was modified by drop coating techniques. CV's were run in the three electrode system (GCE as working electrode, SCE as reference electrode and Pt wire as counter electrode) containing 0.2 M phosphate buffer solution (PBS).

### Results and discussion

XRD patterns of the NiO nanoparticles calcined at

450 °C, was shown in Fig. 1. It demonstrates that they are ordered crystalline and sharp peak, which was indication of higher crystalline nature of the calcined NiO. The sharp diffraction peak in the pattern can be exactly indexed to monoclinic structure of NiO (JCPDS card No. 89-7131) with cell constant  $a = 4.193 \text{ \AA}$ . No characteristic peaks of impurity were detected. The average crystallite size of NiO was determined using Scherrer relation, and was calculated to be around 55 nm. The crystallite size was calculated using the Scherrer formula,  $D = 0.9\lambda/\beta \cos \theta$ . From the diffraction pattern, the diffraction peaks with corresponding planes are at  $2\theta = 37.28^\circ$  (110),  $43.33^\circ$  (200),  $62.96^\circ$  (111). The SEM image of the NiO nanospheres calcined at 450 °C was given below in Fig. 1 (inset). The image demonstrates that the particles adopt irregular morphology with different sized particle due to aggregation. The close examination of SEM image shows that the nanospheres were agglomerated with other spheres, which makes larger particle.

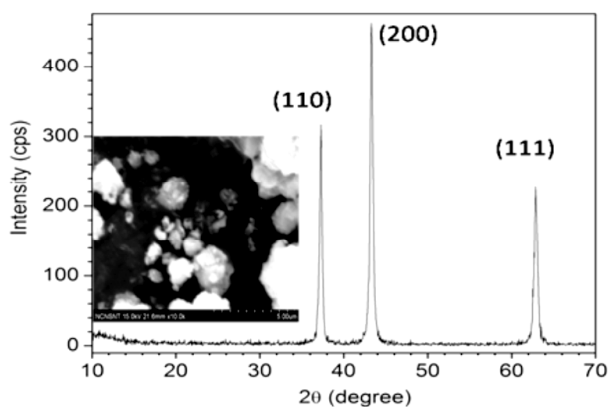


**Fig. 1.** X-Ray diffraction pattern of NiO. Inset : SEM image of NiO nanospheres.

FTIR spectrum of NiO (Fig. 2) showed significant peaks at 3420, 1619 and 451  $\text{cm}^{-1}$ . The sharp absorption band at 451  $\text{cm}^{-1}$  was assigned to Ni-O stretching vibration. Fig. 2 reveals that the broad band centered at 3420  $\text{cm}^{-1}$  was characteristic to the O-H stretching vibration and the weak band at 1619  $\text{cm}^{-1}$  was assigned to H-O-H bending vibration mode. These observations provided the evidence for the presence of hydration in the structure<sup>5</sup>.

Fig. 3 (a), (b) and (c) depicts the cyclic voltammogram (CV) of bare GCE without  $\text{H}_2\text{O}_2$ , GCE/ $\text{H}_2\text{O}_2$  and NiO/GCE/ $\text{H}_2\text{O}_2$  in 0.2 M PBS at 50  $\text{mV s}^{-1}$  respectively. The voltammogram (a) clearly indicates that there was no re-

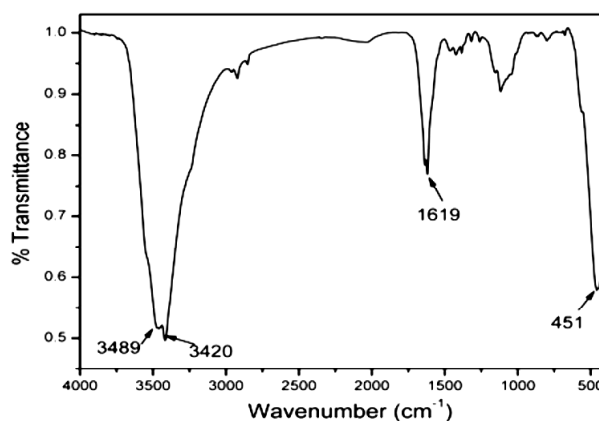


**Fig. 2.** FT-IR spectrum of NiO.

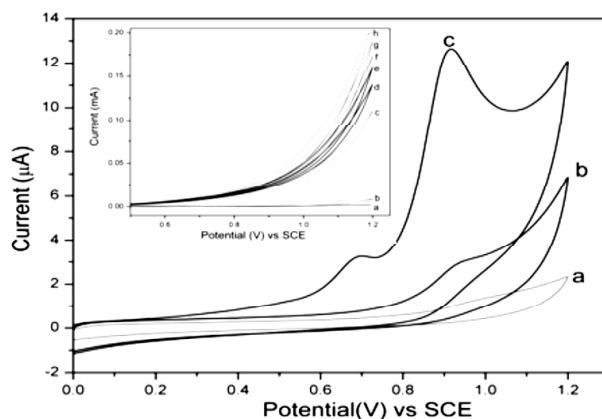


**Fig. 3.** CV of (a) GCE, (b) GCE/ $\text{H}_2\text{O}_2$ , (c) NiO/GCE/ $\text{H}_2\text{O}_2$  and (inset) cyclic voltammetric response at different concentration with 5 mM hydrogen peroxide in 0.2 M buffer at 50  $\text{mV s}^{-1}$ .

dox peak experienced at the GCE in 0.2 M PBS, which indicates that at the potential region of 0 to +1.2 V the GCE was not electroactive. The voltammogram (b) corresponds to the oxidation of 5 mM  $\text{H}_2\text{O}_2$  at the GCE (anodic peak potentials : +0.7, 0.9 V) and the voltammogram (c) corresponds to the anodic oxidation of 5 mM  $\text{H}_2\text{O}_2$  at the NiO/GCE (anodic peak potentials : +0.7, 0.9 V), respectively. The NiO/GCE provides high peak current than the bare GCE, which indicates the electrocatalytic ability of the NiO nanoparticles.

The electrocatalytic ability of the modified electrode was due to the larger available surface area of the modified layer (nanoscale particles)<sup>6</sup>. From the Fig. 3, it is clear that the current response for NiO/GCE was higher than that of bare GCE. From this, it can be concluded that the NiO/GCE can enhance electro-oxidation of  $\text{H}_2\text{O}_2$

in the selected potential range. Fig. 3 (inset) shows the voltammograms of NiO/GCE with different concentration of 1 M H<sub>2</sub>O<sub>2</sub> in 0.2 M phosphate buffer at 50 mV s<sup>-1</sup>. The enhanced anodic current was attributed due to the oxidation of H<sub>2</sub>O<sub>2</sub>. The gradual increase in anodic oxidation peak was due to the addition of 1 M H<sub>2</sub>O<sub>2</sub><sup>7</sup>. It indicates the conducting nature of NiO film on GCE.

### Conclusion

The NiO nanoparticle obtained from Ni-EDTA complex was characterized by XRD and FT-IR spectroscopy. The morphology of NiO powder was studied by SEM analysis. Both Scherrer formula and SEM analysis showed that the spheres were in nanometer scale. The result obtained from the cyclic voltammograms of NiO nanospheres display good electrochemical sensing behaviour towards H<sub>2</sub>O<sub>2</sub> than the bare GCE.

### Acknowledgement

The authors acknowledge NCNSNT, University of Madras for the financial assistance in the form of project fellow and SEM measurements.

### References

1. B. T. Raut, S. G. Pawar, M. A. Chougule, Shashwati Sen and V. B. Patil, *J. Alloys Compd.*, 2011, **50**, 9065.
2. K. Sakuma, K. Miyajima and F. Mafune, *J. Phys. Chem. (A)*, 2013, **117**, 3260.
3. T. Ahmad, K. V. Ramanujachary, S. E. Lofland and A. K. Ganguli, *Solid State Sci.*, 2006, **8**, 425.
4. Y. Ren, W. K. Chim, L. Guo, H. Tanoto, J. Pan and S. Y. Chiam, *Sol. Energy Mater. Sol. Cells*, 2013, **116**, 83.
5. V. Biju and M. Abdul Khadar, *Spectrochim. Acta, Part A*, 2003, **59**, 121.
6. R. Manigandan, K. Giribabu, R. Suresh, L. Vijayalakshmi, A. Stephen and V. Narayanan, *Chem. Sci. Trans.*, 2013, **2(S1)**, 47.
7. A. Salimi, R. Hallaj, S. Soltanian and H. Mamkhezri, *Anal. Chim. Acta*, 2007, **594**, 24.